

# Quantitative evaluation of insulin-induced abdominal subcutaneous dystrophic tissue using shear wave elastography

Genki Sato<sup>1</sup>, Hiroshi Uchino<sup>1\*</sup> , Yosuke Shimizu<sup>2</sup>, Junko Tatebe<sup>3</sup>, Toshisuke Morita<sup>3</sup>, Takahisa Hirose<sup>1</sup>

<sup>1</sup>Division of Diabetes, Metabolism and Endocrinology, Department of Internal Medicine, Toho University Graduate School of Medicine, Tokyo, Japan, <sup>2</sup>Department of Dermatology, Faculty of Medicine, Toho University, Tokyo, Japan, and <sup>3</sup>Department of Laboratory Medicine, Faculty of Medicine, Toho University, Tokyo, Japan

## Keywords

Diabetes, Shear wave elastography, Ultrasound

## \*Correspondence

Hiroshi Uchino  
 Tel.: +813-3762-4151  
 Fax: +813-3765-6488  
 E-mail address:  
 h.uchino@med.toho-u.ac.jp

*J Diabetes Investig* 2022; 13: 1004–1010

doi:10.1111/jdi.13762

## ABSTRACT

**Aims/Introduction:** Subcutaneous dystrophic tissue (DT) produced by insulin injection causes dysglycemia owing to inadequate absorption of insulin. However, precise techniques for measuring DT have not been established. Shear wave elastography (SWE) is an imaging technology that can quantify tissue stiffness. In this study, insulin injection-induced DT was quantified using SWE to generate whole-abdominal wall subcutaneous tissue by three-dimensional (3D) imaging in patients with type 2 diabetes who were treated with multiple insulin injections.

**Materials and Methods:** Seven patients with type 2 diabetes were recruited who received long-standing multiple insulin injections. Using SWE, the shear wave velocity (SWV) of DT and control (normal subcutaneous tissue) was measured. Furthermore, two of seven patients underwent whole-abdominal SWE examination to calculate the proportion of DT. A subcutaneous insulin tolerance test was also performed in both the DT and control tissues.

**Results:** The SWV in DT was significantly higher than that in the control tissue (2.87 [2.66–2.98] vs 1.29 [1.23–1.44] m/s,  $P < 0.01$ ). The proportion of the DT volume was 0.67% and 5.21% for two individuals from the entire abdominal subcutaneous tissue volume. The area under the curve for the subcutaneously injected insulin aspart concentration at the DT sites was lower than that of the control tissue (75.0 [52.1–111] vs 116 [86.9–152.5] h\*mU/L,  $P = 0.1$ ).

**Conclusions:** SWE can be useful in quantifying abdominal subcutaneous insulin-induced DT, especially the 3D volume of insulin injection-induced DT from the entire abdominal subcutaneous tissue. This study is the first to examine the volume and distribution of abdominal subcutaneous DT using SWE.

## INTRODUCTION

Insulin is a hormone that is commonly administered through a subcutaneous injection and has been used widely for blood glucose management in type 1 and 2 diabetes. Insulin therapy aims to mimic the physiological concentration of insulin; however, insulin absorption by the subcutaneous tissue can vary based on the preparation, injection technique, and injection site<sup>1–6</sup>. Variability in the subcutaneous absorption of insulin is

related to glucose variability and can arise as an unpredictable therapeutic response, resulting in inadequate glycemic control and an increased risk of hypoglycemia<sup>1,7</sup>. Some studies have shown that subcutaneous injections of insulin may cause dystrophic tissue such as lipohypertrophy, fibrocollagenous scars, and insulin-derived amyloidosis in patients with diabetes<sup>2,8–12</sup>. In addition, dystrophic tissue can cause poor blood glycemic control due to the inadequate absorption of insulin<sup>2,8–11,13,14</sup>. Despite undergoing frequent abdominal subcutaneous tissue investigations, many patients with multiple insulin injections have fluctuations in blood glucose levels and experience severe

Received 5 November 2021; revised 10 January 2022; accepted 27 January 2022

hypoglycemia. Therefore, a non-invasive and examiner-independent method with improved diagnostic accuracy is needed to assess the condition of the subcutaneous abdominal tissue.

Subcutaneous dystrophic tissue is typically diagnosed based on clinical evidence of a palpable subcutaneous lump and confirmed by pathological examination<sup>11,15–22</sup>. However, a standard technique to quantify the amount of dystrophic tissue has not yet been established thus far. Tissue stiffness is associated with underlying pathological states. Thus, the measurement of tissue stiffness may be a useful clinical estimation of the severity of tissue pathology. Ultrasound elastography is an imaging technology that is sensitive to tissue stiffness, and it was first described in the 1990s<sup>23</sup>. Strain elastography was the first ultrasound elastography technique<sup>24</sup>. Although strain elastography can represent strain measurements as a semitransparent color map overlaid on a B-mode image, it is not usually quantifiable. In contrast to strain elastography, shear wave elastography (SWE) can produce quantitative images of shear wave velocity (SWV). Measurement of SWV yields both qualitative and quantitative estimates of tissue elasticity<sup>25</sup>. In general, the stiffer the tissue, the greater is the SWV. In addition, SWV has high user-independence and reproducibility, and thus, SWE has the advantage of quantifying superficial tissue stiffness. In this study, SWE was used to evaluate quantitatively abdominal subcutaneous dystrophic tissue in patients with type 2 diabetes who were treated with multiple insulin injections.

## MATERIALS AND METHODS

### Study design

A single-center observational proof-of-principle study was conducted to examine the characteristics of subcutaneous dystrophic tissue generated by daily insulin injections in patients with type 2 diabetes.

### Participants

Outpatients were enrolled with type 2 diabetes who received daily insulin injections at Toho University Omori Medical Center, Tokyo. Patients were enrolled between December 2018 and December 2019 and provided informed consent. Our eligibility criteria included suspicion of subcutaneous dystrophic tissue at the insulin injection site and age  $\geq 20$  years. Patients were excluded with heart failure, a history of heart failure, a medical history of hypersensitivity to any of the ingredients of the study drugs, severe ketosis, diabetic coma or pre-coma, severe liver dysfunction, severe renal dysfunction, serious infectious disease, pre- or post-operative state, and serious injury and those receiving cancer treatment. Seven patients who met these criteria were enrolled in this study.

### Setting

The SWV was measured (in m/s) using the Virtual Touch™ Imaging Quantification (VTIQ) mode with Acuson S3000™ and a 9L4 probe (6.5 MHz  $\pm$  20%) (Siemens Medical Solutions, Mountain View, CA, USA) (Figure S1). We embedded a 0.5

cm thick spacer (Yasojima Proceed Co., Ltd, Osaka, Japan) between the skin surface and the ultrasound probe to mitigate the shear wave signal error. The team for each examination consisted of an examiner and a recorder.

### Comparison between the subcutaneous dystrophic tissue and the control tissue

Two independent investigators confirmed the presence of subcutaneous lumps at the site of repetitive insulin injections through visible inspection and palpation<sup>22</sup>. A palpable subcutaneous lump was classified as dystrophic tissue, and the lateral abdominal normal adipose tissue of the same subject was classified as the control tissue. Raw SWV data were obtained using a standard protocol, according to the manufacturer's recommendations (Virtual Touch™ Image Quantification by Siemens). The region of interest (ROI) included the dystrophic and control tissues, which served as the control-specific background values (Figure S1). Three different ROIs were selected at the site of the insulin injection and control regions. SWV was measured at these ROIs, and the mean SWV was calculated in m/s. Two or three independent reviewers analyzed the data from these samples to assess the reliability and to reduce the bias associated with the placement of the dystrophic tissue and control ROIs. The SWV was compared between the dystrophic tissue and control tissue using the Mann-Whitney *U* test.

### Proportion of dystrophic tissue in the abdominal wall

Two patients underwent an entire abdominal SWE examination to evaluate the entire abdominal subcutaneous tissue. The entire abdominal surface area was assessed as a vertical axis between the lower costal margin and the superior anterior iliac spine and as a horizontal axis between both anterior axillary lines. The VTIQ images were obtained with 1 cm step size intervals toward the cranial-to-caudal axis governed by a 2 cm working distance in the horizontal axis (Figure S2). The ROIs were defined as 4 cm  $\times$  4 cm areas, and each superior margin was mapped to the surface of the epidermis. To reconstruct three-dimensional (3D) full-length horizontal abdominal VTIQ images, the individual VTIQ image stacks were rendered by a working distance of 1 cm to cover each edge of the image. Imaging analysis was performed using Dragonfly software (Montreal, Quebec, Canada). The superior and inferior margins of the subcutaneous tissue were set as the dermis and fascia, respectively. The colored RGB (red-green-blue) images of VTIQ at the ROIs were changed to SWV data according to the manufacturer's guidelines, using adaptive histogram equalization. The amount of whole-abdominal dystrophic tissue was calculated using the following equation: percentage of dystrophic tissue = total dystrophic tissue SWV density number/entire subcutaneous tissue area density number. The SWV density numbers were calculated using the SWV histogram. The average of three individual SWV data derived from the dystrophic and control tissues were calculated and each data point was used as the upper and lower margins of the SWV histogram

cutoff points to account for the dystrophic tissue and the entire abdominal subcutaneous tissue, respectively. The distribution of the high SWV area was also evaluated throughout the abdominal wall.

### Subcutaneous insulin tolerance test

Patients arrived at our institution in the morning after an overnight fast and skipped their morning bolus of insulin. To compare insulin absorption, the patients received subcutaneous abdominal injections of 0.1 unit/standard body weight (kg) of insulin aspart (IAsp) into the dystrophic tissue and control sites. Blood samples were collected before the insulin injection and at every 30 min for up to 240 min after the injection. Serum iso-insulin (Mercodia AB, Uppsala, Sweden) and human insulin (Roche Diagnostics, Tokyo, Japan) levels were measured, and the serum IAsp concentration was determined using the following formula: serum IAsp concentration (mU/L) = (serum iso-insulin) – (serum human insulin). The area under the curve of serum IAsp concentration values from 0 to 240 min ( $AUC_{IAsp}$ ) was calculated using the trapezoidal method. The  $AUC_{IAsp}$  after administering insulin injections into the dystrophic tissue vs control sites was compared using the Mann-Whitney *U* test.

### Statistical analysis

All statistical analyses were conducted using JMP, version 13.0.0. The data are shown as median (interquartile range). The Mann-Whitney *U* test was used to compare values between the subcutaneous dystrophic tissue and control tissue, with the level of significance set at  $P < 0.05$ .

## RESULTS

### Patient characteristics

Table 1 presents the baseline characteristics of the patients. The study population comprised four (57%) men and three (43%) women, with a median age of 64 (56–70) years. The body mass

index was 29.4 (27.5–33.0) kg/m<sup>2</sup>, and the HbA1c was 7.9 (7.4–9.1)%. The duration of diabetes was 22 (20–25) years, and the duration of insulin therapy was 9 (6–23) years. All patients had been using insulin analogs for multiple daily insulin injections, and the total daily insulin dose was 64 (38–79) U/day.

### Comparison of stiffness between the dystrophic and control tissues

The SWV of the dystrophic and control tissues is also shown in Table 1. The SWV of the dystrophic tissue was significantly higher than that of the control tissue (2.87 [2.66–2.98] vs 1.29 [1.23–1.44] m/s,  $P < 0.01$ ).

### Proportion of dystrophic tissue in the whole abdominal wall

Figure 1 shows the SWE histogram and the percentage of dystrophic tissue. The density of dystrophic tissue/entire subcutaneous tissue area was 39,783/5,894,523 pixels in patient 4, and 194,481/3,730,419 in patient 7, respectively. Therefore, each proportion of dystrophic tissue volume calculated from the entire subcutaneous abdominal tissue was 0.67% and 5.21%. Whole-abdominal 3D-VTIQ images highlighted the presence of some high SWV lesions during the entire subcutaneous abdominal scanning (Figure 1c), which were undiagnosed as dystrophic tissue before the examination.

### Subcutaneous insulin tolerance test

Five of the seven patients' subcutaneous insulin tolerance test data were available. Data from two patients were excluded because of data errors and lack of specimen collection. Figure 2 shows the boxplots of the serum IAsp concentration ( $AUC_{IAsp}$ ) over time after administering IAsp injection into areas with the dystrophic and control tissues. Although not significant, the insulin subcutaneous absorption tended to be lower after injection at the dystrophic tissue site than after injection at the control site (75.0 [52.1–111] vs 116 [86.9–152.5] h\*mU/L,  $P = 0.0947$ ).

**Table 1** | Patients' baseline characteristics and shear wave velocity of dystrophic and control tissues

Characteristic	Patient 1	Patient 2	Patient 3	Patient 4	Patient 5	Patient 6	Patient 7	Median (IQR)
Age (years)	43	67	58	70	77	56	64	64 (56–70)
Sex	F	F	M	M	M	F	M	
BW (kg)	71.2	63.2	103.4	75.2	76.9	82.5	71.3	75.2 (71.2–82.5)
BMI (kg/m <sup>2</sup> )	30.8	28.5	40.4	29.4	27.2	33	27.5	29.4 (27.5–33.0)
Duration of diabetes (years)	22	20	10	22	28	25	21	22 (20–25)
HbA1c (%)	9.5	9.1	7.9	7.4	8.8	7.6	6.6	7.9 (7.4–9.1)
Duration of insulin use (years)	6	10	8	23	35	5	9	9 (6–23)
Number of daily insulin injections	4	4	4	4	4	4	4	4
Daily insulin dose (unit/day)	79	64	106	42	74	32	38	64 (38–79)
Daily insulin dose (unit/kg/day)	1.11	1.01	1.03	0.56	0.96	0.39	0.53	0.96 (0.53–1.03)
SWV (dystrophic tissue) (m/s)	2.87	2.66	2.79	3.27	2.98	2.97	2.53	2.87 (2.66–2.98)*
SWV (control) (m/s)	1.5	1.2	1.28	1.23	1.41	1.44	1.29	1.29 (1.23–1.44)

BMI, body mass index; BW, body weight; SWV, shear wave velocity, IQR, interquartile range. \* $P < 0.01$ ; *P* value is reported for the Mann-Whitney *U* test, comparing the SWV between the dystrophic tissue and the control tissue.

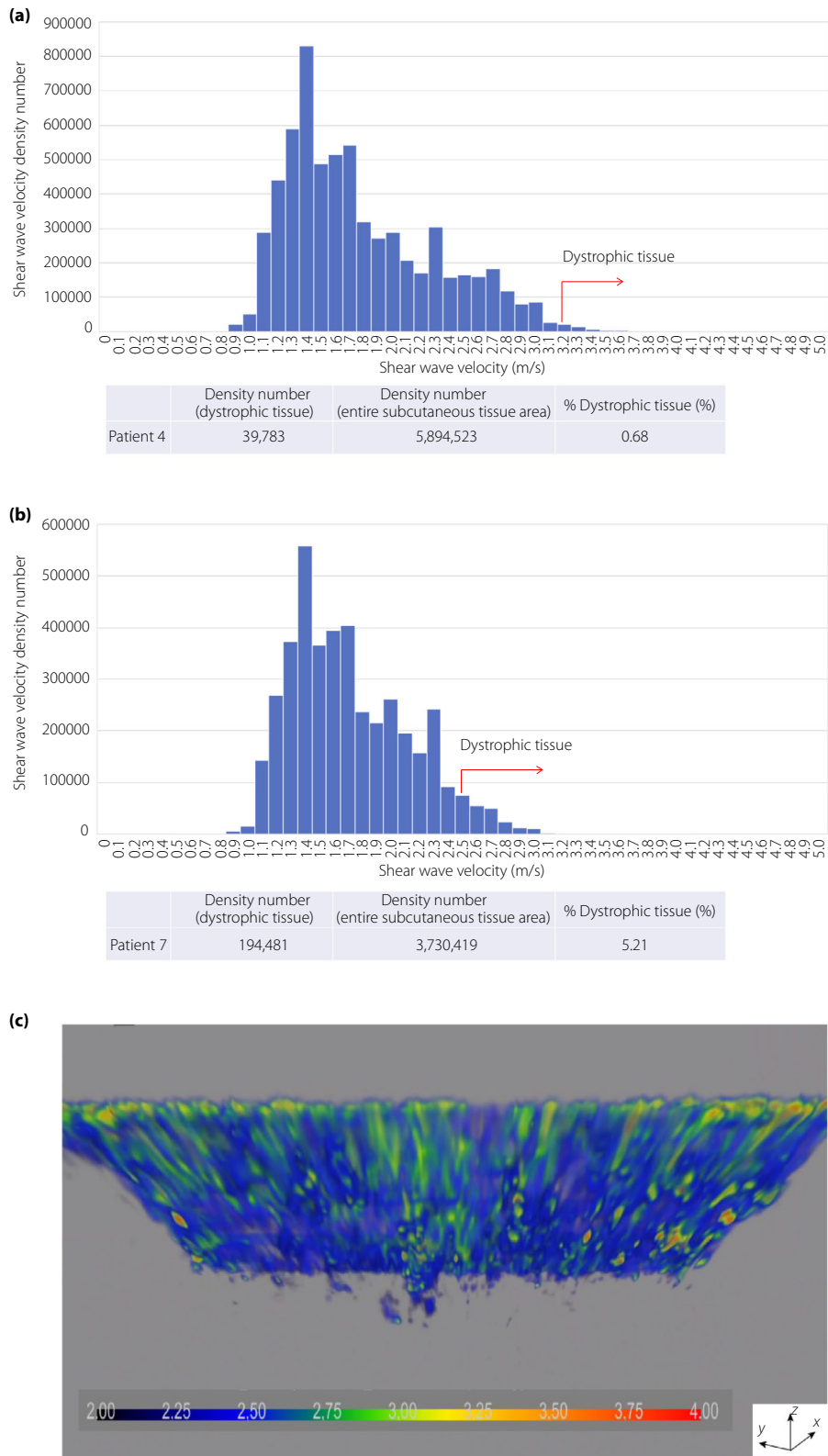


**Figure 1** | Histogram of the individual shear wave velocity density numbers and percentage dystrophic tissue and the measured 3D whole-abdominal subcutaneous tissue. The figure shows a histogram of the individual shear wave velocity (SWV) density numbers and % dystrophic tissue. Upper (a) and lower (b) histograms depict the data of patients 4 and 7 within the 3D whole-abdominal wall examination, respectively. 3D whole-abdominal subcutaneous tissue image by SWE of patient 4 (c). The color scale indicates the shear wave velocity (m/s). The x, y, and z directions represent head-to-tail, left-to-right, and inner-to-outer, respectively.

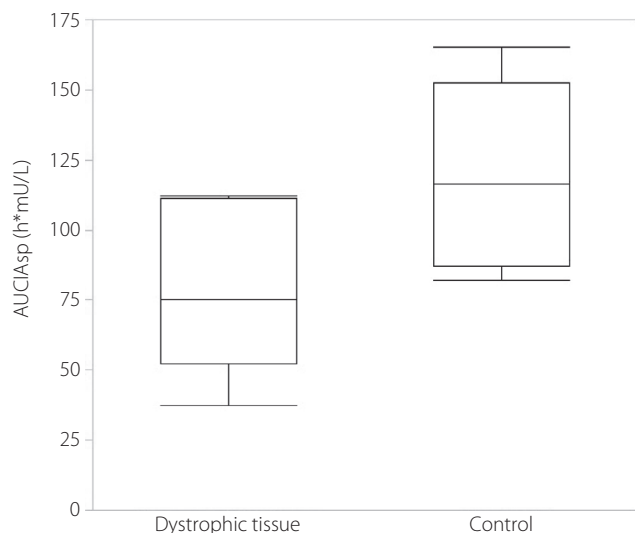


**Figure 2** | Boxplots of the area under the curve of serum insulin aspart (IAsp) concentration ( $AUC_{IAsp}$ ) over time after IAsp injection into areas with dystrophic and control tissues. The figure shows the boxplots of the area under the curve of serum IAsp concentration ( $AUC_{IAsp}$ ) over time after IAsp injection into areas with dystrophic and control tissues.

## DISCUSSION

In this study, it was found that the SWV of the insulin injection-induced dystrophic tissue was significantly higher than that of the control tissue ( $P < 0.01$ ). In addition, the volumes of the dystrophic tissue were 0.67% and 5.21% of the entire abdominal subcutaneous tissue in sample subjects. The subcutaneous insulin absorption was lower at the dystrophic tissue sites than at the control sites, with a marginal difference ( $P = 0.0947$ ).

Insulin injection-induced subcutaneous dystrophic tissue, such as lipohypertrophy, fibrotic scar tissue, or amyloid tissue, has been traditionally assessed only by survey or physical examination. Previous studies have reported that palpable lumps were not observed in all cases of insulin amyloid<sup>26</sup>. Thus, it is difficult to identify dystrophic tissue only by physical examination. Some authors reported that subcutaneous dystrophic tissue caused by insulin injections, which could be identified by physical examination, could also be detected by ultrasound<sup>27,28</sup>. Furthermore, another study showed that ultrasound could be used to detect cases wherein subcutaneous lesions were not identified by physical observation<sup>29</sup>. However, it remains unclear how widespread insulin injection-induced abdominal subcutaneous dystrophic tissue has been distributed throughout the subcutaneous abdominal wall. To the best of our knowledge, this is the first study to examine the volume and distribution of abdominal subcutaneous dystrophic tissue using SWE. Previous studies have shown that all types of dystrophic tissue, such as lipohypertrophy, fibrotic scars, and amyloid at the site of insulin injection, inhibit insulin absorption<sup>2,8,10,11</sup>. In agreement with the findings of previous reports, our study showed that insulin

absorption after administering injections into dystrophic tissue sites was reduced when compared with that after administering injections into the control sites. However, the difference was not significant ( $P = 0.0947$ ). This result could be attributed to the small number of cases.

Our results showed that the SWV of the insulin injection-induced dystrophic tissue was higher than that of the normal adipose tissue. These data may reflect histopathological changes such as fibrosis and amyloid deposits. Although it is necessary to perform histopathological examination to prove our hypothesis, the dystrophic tissue occupied only 0.67% and 5.21% of the volume of the entire abdominal subcutaneous tissue in the sample subjects. Thus, our methods could be useful for more precise identification of dystrophic tissue areas. These data suggest that there are lesions other than palpable subcutaneous lumps where repeated insulin injections are administered. Previous studies have shown that non-palpable lesions that are difficult to detect by physical diagnosis are also related to an insulin absorption disorder<sup>29</sup>. Thus, it is important to detect subcutaneous dystrophic tissue to achieve normal insulin delivery and good glycemic control.

## Limitations

This study had several limitations. First, the number of cases was small, particularly in the whole abdominal study, wherein only two patients were included. Second, we regarded palpable subcutaneous lumps as dystrophic tissue and defined the average SWV of three different ROIs as the reference value of the dystrophic tissue. However, a previous study that used strain elastography reported that the palpable dystrophic tissue was harder than the non-palpable type<sup>29</sup>. Thus, the non-palpable dystrophic tissue may have been overlooked in our method. Additional studies are needed to determine whether non-palpable dystrophic tissue has a lower SWV than the palpable type. Third, we did not perform any pathological examination in our study. Thus, we were unable to prove whether the high SWV was histologically associated with pathological changes such as lipohypertrophy, fibrotic lesions, and amyloid. Finally, it was difficult to show clearly the cutoff value of SWV that separated the dystrophic tissue from the normal tissue because the number of cases was small. Further large-scale studies are necessary to differentiate quantitatively between the dystrophic tissue and the normal tissue using SWE.

A quantitative evaluation of insulin injection-induced subcutaneous tissue changes was performed using SWE. The SWV of the insulin injection-induced dystrophic tissue was significantly higher than that of normal adipose tissue. Our findings showed that SWE enables the calculation of the 3D volume of the insulin injection-induced dystrophic tissue from the entire abdominal subcutaneous tissue. Although there was no significant difference, the insulin subcutaneous absorption was slower in the dystrophic tissue than in the normal adipose tissue. In the future, we intend to validate our system with a larger number of patients and using automated 3D-imaging software.

**ACKNOWLEDGMENTS**

We thank K. Okui and M. Suzuki for their assistance in obtaining approval from the local ethics committee for the experiments and for providing analysis computers, software, and advice. We would like to thank Editage (www.editage.com) for English language editing.

This work was supported by funding from the Grant-in-Aid for Scientific Research from the Japan Science and Technology Agency, KAKEN (17K01425 and 20K12579, JSPS).

**DISCLOSURE**

The authors declare no conflict of interest.

Approval of the research protocol: The Ethics Committee of the Faculty of Medicine, Toho University, Tokyo, Japan, approved all the procedures performed in this study (No. A18125).

Informed consent: Written informed consent was obtained from all the participants.

Approval date of registry and the registration no. of the study/trial: The study was approved on April 12, 2018, (No. A18125).  
Animal studies: N/A.

**REFERENCES**

- Gin H, Hanaire-Broutin H. Reproducibility and variability in the action of injected insulin. *Diabetes Metab* 2005; 31: 7–13. [https://doi.org/10.1016/s1262-3636\(07\)70160-x](https://doi.org/10.1016/s1262-3636(07)70160-x)
- Famulla S, Hövelmann U, Fischer A, et al. Insulin injection into lipohypertrophic tissue: blunted and more variable insulin absorption and action and impaired postprandial glucose control. *Diabetes Care* 2016; 39: 1486–1492. <https://doi.org/10.2337/dc16-0610>
- Pozzuoli GM, Laudato M, Barone M, et al. Errors in insulin treatment management and risk of lipohypertrophy. *Acta Diabetol* 2018; 55: 67–73. <https://doi.org/10.1007/s00592-017-1066-y>
- Braak EWT, Woodworth JR, Bianchi R, et al. Injection site effects on the pharmacokinetics and glucodynamics of insulin lispro and regular insulin. *Diabetes Care* 1996; 19: 1437–1440. <https://doi.org/10.2337/diacare.19.12.1437>
- Frid A, Linde B. Intraregional differences in the absorption of unmodified insulin from the abdominal wall. *Diabetes Med* 1992; 9: 236–239. <https://doi.org/10.1111/j.1464-5491.1992.tb01768.x>
- Frid AH, Kreugel G, Grassi G, et al. New insulin delivery recommendations. *Mayo Clin Proc* 2016; 91: 1231–1255. <https://doi.org/10.1016/j.mayocp.2016.06.010>
- Vora J, Heise T. Variability of glucose-lowering effect as a limiting factor in optimizing basal insulin therapy: a review. *Diabetes Obes Metab* 2013; 15: 701–712. <https://doi.org/10.1111/dom.12087>
- Blanco M, Hernández MT, Strauss KW, et al. Prevalence and risk factors of lipohypertrophy in insulin-injecting patients with diabetes. *Diabetes Metab* 2013; 39: 445–453. <https://doi.org/10.1016/j.diabet.2013.05.006>
- Nagase T, Katsura Y, Iwaki Y, et al. The insulin ball. *Lancet* 2009; 373: 184. [https://doi.org/10.1016/S0140-6736\(09\)60041-6](https://doi.org/10.1016/S0140-6736(09)60041-6)
- Wallymahmed ME, Littler P, Clegg C, et al. Nodules of fibrocollagenous scar tissue induced by subcutaneous insulin injections: a cause of poor diabetic control. *Postgrad Med J* 2004; 80: 732–733. <https://doi.org/10.1136/pgmj.2004.019547>
- Nagase T, Iwaya K, Iwaki Y, et al. Insulin-derived amyloidosis and poor glycemic control: a case series. *Am J Med* 2014; 127: 450–454. <https://doi.org/10.1016/j.amjmed.2013.10.029>
- Ji L, Sun Z, Li Q, et al. Lipohypertrophy in China: prevalence, risk factors, insulin consumption, and clinical impact. *Diabetes Technol Ther* 2017; 19: 61–67. <https://doi.org/10.1089/dia.2016.0334>
- Johansson U-B, Amsberg S, Hannerz L, et al. Impaired absorption of insulin aspart from lipohypertrophic injection sites. *Diabetes Care* 2005; 28: 2025–2027. <https://doi.org/10.2337/diacare.28.8.2025>
- Heinemann L. Insulin absorption from lipodystrophic areas: a (neglected) source of trouble for insulin therapy? *J Diabetes Sci Technol* 2010; 4: 750–753. <https://doi.org/10.1177/193229681000400332>
- Ansari AM, Osmani L, Matsangos AE, et al. Current insight in the localized insulin-derived amyloidosis (LIDA): clinicopathological characteristics and differential diagnosis. *Pathol Res Pract* 2017; 213: 1237–1241. <https://doi.org/10.1016/j.prp.2017.08.013>
- Samlaska C, Reber S, Murry T. Insulin-derived amyloidosis: The insulin ball, amyloidoma. *JAAD Case Rep* 2020; 6: 351–353. <https://doi.org/10.1016/j.jidcr.2020.02.011>
- Grunes D, Rapkiewicz A, Simsir A. Amyloidoma secondary to insulin injection: cytologic diagnosis and pitfalls. *Cytojournal* 2015; 12: 15. <https://doi.org/10.4103/1742-6413.161602>
- Mayhew JM, Alan T, Kalidindi V, et al. Isolated insulin-derived amyloidoma of the breast. *BMJ Case Rep* 2017; 2017: bcr2017219491. <https://doi.org/10.1136/bcr-2017-219491>
- Mangla A, Kim GJ, Agarwal N, et al. Localized insulin amyloidosis with use of concentrated insulin: a potential complication. *Diabetes Med* 2016; 33: e32–e35. <https://doi.org/10.1111/dme.13137>
- Shikama Y, Kitazawa J-I, Yagihashi N, et al. Localized amyloidosis at the site of repeated insulin injection in a diabetic patient. *Intern Med* 2010; 49: 397–401. <https://doi.org/10.2169/internalmedicine.49.2633>
- Yumlu S, Barany R, Eriksson M, et al. Localized insulin-derived amyloidosis in patients with diabetes mellitus: a case report. *Hum Pathol* 2009; 40: 1655–1660. <https://doi.org/10.1016/j.humpath.2009.02.019>

22. Gentile S, Guarino G, Giancaterini A, *et al.* A suitable palpation technique allows to identify skin lipohypertrophic lesions in insulin-treated people with diabetes. *Springerplus* 2016; 5: 563–569. <https://doi.org/10.1186/s40064-016-1978-y>
23. Gennisson J-L, Deffieux T, Fink M, *et al.* Ultrasound elastography: principles and techniques. *Diagn Interv Imaging* 2013; 94: 487–495. <https://doi.org/10.1016/j.diii.2013.01.022>
24. Ophir J, Céspedes I, Ponnekanti H, *et al.* Elastography: a quantitative method for imaging the elasticity of biological tissues. *Ultrason Imaging* 1991; 13: 111–134. <https://doi.org/10.1177/016173469101300201>
25. Sigrist RMS, Liao J, Kaffas AE, *et al.* Ultrasound elastography: review of techniques and clinical applications. *Theranostics* 2017; 7: 1303–1329. <https://doi.org/10.7150/thno.18650>
26. D'Souza A, Theis JD, Vrana JA, *et al.* Localized insulin-derived amyloidosis: a potential pitfall in the diagnosis of systemic amyloidosis by fat aspirate. *Am J Hematol* 2012; 87: E131–132. <https://doi.org/10.1002/ajh.23334>
27. Perciun R. Ultrasonographic aspect of subcutaneous tissue dystrophies as a result of insulin injections. *Med Ultrason* 2010; 12: 104–109.
28. Perciun R, Telcian A, Olariu L. Ultrasound assessment of cutaneous/subcutaneous dystrophies in insulin-treated patients. A report on two cases. *Med Ultrason* 2012; 14: 60–63.
29. Kikuchi M, Hirokawa N, Hagiwara S, *et al.* Ultrasonography improves glycemic control by detecting insulin-derived localized amyloidosis. *Ultrasound Med Biol* 2017; 43: 2284–2294. <https://doi.org/10.1016/j.ultrasmedbio.2017.06.011>

## SUPPORTING INFORMATION

Additional supporting information may be found online in the Supporting Information section at the end of the article.

**Figure S1** | Depiction of the abdominal subcutaneous dystrophic tissue using shear wave elastography.

**Figure S2** | Entire abdominal shear wave elastography examination.